Available online at www.sciencedirect.com
ScienceDirect
Geochimica et Cosmochimica Acta 71 (2007) 2657–2671
Geochimica et Cosmochimica Acta
www.elsevier.com/locate/gca

Experimental and numerical studies of the ^{18}O exchange between CO_2 and water in the atmosphere–soil invasion flux

Yaacov Kapiluto [a], Dan Yakir [a,*], Pieter Tans [b], Brian Berkowitz [a]

[a] *Department of Environmental Sciences and Energy Research, Weizmann Institute of Science, Rehovot 76100, Israel*
[b] *Climate Monitoring and Diagnostics Laboratory, NOAA, Boulder, CO 80305, USA*

Received 21 August 2006; accepted in revised form 22 March 2007; available online 28 March 2007

Abstract

The $^{18}O/^{16}O$ ratio of CO_2 is a potentially powerful tracer of carbon dioxide fluxes from the soil to the atmosphere, which is influenced by complex interactions involving both biotic and abiotic soil processes. We use a simplified experimental approach and numerical simulations to examine in isolation the ^{18}O exchange between CO_2 and soil water associated with the abiotic *invasion* of atmospheric CO_2 into soil. This allowed us to verify, in particular, whether the ^{18}O of the retro-diffusion flux of CO_2 from the soil reflects ^{18}O equilibration with water at the soil surface, or at some depth. Sterile soil samples with known water isotopic composition were placed in a closed box attached to a specially designed flow chamber and the changes in $\delta^{18}O$ of CO_2 between the chamber inlet and outlet, due only to *invasion* effects, were determined. Numerical simulations constrained by the laboratory gas exchange measurements indicated that between the two commonly used diffusion models [Penman, H.L. (1940). Gas and vapor movements in soil, 1: the diffusion of vapors through porous solids. *Int. J. Agric. Sci.* **30**, 437–462; Moldrup, P., Olesen, T., Yamaguchi, T., Schjonning, P., Rolston, D.E. (1999). Modeling diffusion and reaction in soils, IX, the Backingham–Burdine–Campbell equation for gas diffusivity in undisturbed soil. *Soil Sci.* **164**, 542–551], only the former provided good agreement with the measurements over a wide range of soil water contents. Based on the model calculations constrained by experimental data, and on comparison of characteristic diffusion/reaction times, we conclude that the depth required for full CO_2–water ^{18}O equilibration ranges between 2 and 8.5 cm. The depth depends, in order of importance, on (1) soil moisture content; (2) temperature, which dominates the rate of hydration isotopic exchange; (3) CO_2 residence time, which is determined by the time of replacement of the column air above the soil; and (4) soil structure, including porosity, tortuosity and grain size, with the later probably influencing the water surface area exposed to CO_2 exchange. Using field data from a semi-arid forest site in Israel, numerical simulations indicated that the ^{18}O full equilibrium depth varied at this site between 4 cm (January) and 8 cm (November), being sensitive mostly to temperature and soil water content. Deepening of the equilibration depth as the soil dries should limit the effects of ^{18}O evaporative enrichment at the surface on the isotopic composition of the soil–atmosphere CO_2 flux.
© 2007 Elsevier Ltd. All rights reserved.

1. INTRODUCTION

1.1. The use of stable isotopes to study terrestrial CO_2 fluxes

Organic matter in soil is the largest pool of global carbon on land. The annual flux of carbon between soils and the atmosphere is equivalent to nearly 10% of the carbon pool in the atmosphere. Therefore, small variations in the flux can result in significant variations in atmospheric CO_2 concentrations. This is particularly relevant at present when atmospheric CO_2 concentrations are increasing due to human-induced emission of $\sim 7 \times 10^{15}$ g carbon annually (from land use change, deforestation and fossil fuels); these increases are expected to be associated with climatic changes (IPCC 2001). Currently, the growth rate of the atmospheric CO_2 concentration is estimated

* Corresponding author. Fax: +972 8 9344124.
E-mail address: dan.yakir@weizmann.ac.il (D. Yakir).

0016-7037/$ - see front matter © 2007 Elsevier Ltd. All rights reserved.
doi:10.1016/j.gca.2007.03.016

at ~1.5 ppm yr^{-1}, which is equivalent to an annual increase of ~0.4% (www.cmdl.noaa.gov/ccgg/trends). Although assessments of changes in atmospheric CO_2 concentrations indicate changes in the activity of the land biosphere, specific information on sinks or sources of carbon are scarce (Keeling et al., 1996; Randerson et al., 1997; Hemming and Yakir, 2005; see also www.fluxnet.ornl.gov/fluxnet/).

Stable isotopes of CO_2 (^{13}C and ^{18}O) provide a powerful research measure to trace CO_2 fluxes and gain insights to underlying processes. While the use of ^{13}C is relatively well established, the application of ^{18}O in CO_2 to carbon cycle studies is still developing (Yakir, 2003). Francey and Tans (1987) showed the ^{18}O content of atmospheric CO_2 varies latitudinally (and that this large signal must be influenced by CO_2 exchange with the land biosphere). They also showed that variations in the $\delta^{18}O$ value of atmospheric CO_2 are influenced by the markedly different ^{18}O signals associated with photosynthesis and soil respiration, both of which reflect oxygen exchange between CO_2 and water in the respective reservoir (Francey and Tans, 1987; Siegenthaler et al., 1987; Farquhar et al., 1993; Gillon and Yakir, 2001; Yakir and Wang, 1996). However, significant uncertainties are still associated with the ^{18}O signal of soil-respired CO_2 (Miller et al., 1999; Stern et al., 2001; Riley et al., 2003).

The ^{18}O of atmospheric CO_2 is described in the framework of a global mass balance equation such as (e.g., Miller et al., 1999):

$$\begin{aligned}\frac{d\delta_a}{dt} = \frac{1}{C_a}[&F_{oa}(\delta_o - \delta_a) + \varepsilon_w(F_{oa} - F_{ao}) + F_{ff}(\delta_{ff} - \delta_a)\\ &+ F_{bb}(\delta_{bb} - \delta_a) + F_A(\delta_l - \delta_a + \varepsilon_l)\\ &+ F_{sa}(\delta_{eq} - \delta_a + \varepsilon_{eff}) + F_I(\varepsilon_{eq} - \delta_a)]\end{aligned} \quad (1)$$

where $F_A = (C_l/(C_a - C_l))A$ (with $A = F_{la} - F_{al}$, which denotes the photosynthetic carbon assimilation flux), C is the CO_2 concentration, F is flux, δ denotes normalized isotope ratio defined by $\delta = R_{sample}/R_{reference} - 1$, $R = {}^{18}O/{}^{16}O$, and the reference is V-PDB$_{CO_2}$. This latter scale provides good comparison with δ values for water on the V-SMOW due to the similarity of the CO_2–H_2O equilibrium fractionation, and the V-PDB$_{CO_2}$ and V-SMOW differences (Brenninkmeijer et al., 1983; cf. Yakir, 2003). Subscripts represent the reservoir of CO_2 that leaves or enters the atmosphere (a), ocean (o), fossil fuels (ff), biomass burning (bb), leaves (l), and soil (s). The parameter ε refers to the kinetic fractionation associated with fluxes between reservoirs, eq and eff denote the type of isotopic fractionation, where ε_{eq} is defined below Eq. (3) and ε_{eff} represents an effective diffusion fractionation in the soil atmosphere interface (Miller et al., 1999), and I represents an invasion flux of atmospheric CO_2 diffusing into and out of soil (as added to the budget by Miller et al., 1999), which is discussed below in more detail. While many of the parameters used in Eq. (1) can be reasonably well estimated, or their effect on the overall budget is small (cf. Hillel, 1980; Conway et al., 1994; Trolier et al., 1996; Blunier et al., 2002), the isotopic fluxes associated with leaves and soil are the largest and most uncertain. Knowledge of the $\delta^{18}O$ linked to soil and leaf fluxes can help estimate these fluxes individually, which will constitute a significant advance in understanding responses of the contemporary carbon cycle to global change.

1.2. Oxygen isotope ratios of soil CO_2

The primary control on the atmospheric $\delta^{18}O$ of CO_2 is based on hydration of CO_2 and the subsequent exchanges of oxygen atoms (and their isotopes) between CO_2 and water, resulting with ^{18}O exchange according to:

$$H_2{}^{18}O_{(l)} + CO_{2(g)} \Longleftrightarrow H^+ + HCO_2{}^{18}O^-_{(aq)} \Longleftrightarrow H_2O_{(l)} + CO^{18}O_{(g)} \quad (2)$$

While normally the overwhelming quantity of water relative to CO_2 in nature results in water controlling the $\delta^{18}O$ of CO_2 in the system, an equilibrium isotope effect between CO_2 and water exists (Brenninkmeijer et al., 1983):

$$\alpha_{eq}(T) = \frac{[{}^{18}O/{}^{16}O]_{CO_2}}{[{}^{18}O/{}^{16}O]_{H_2O}} \quad (3)$$

often expressed as $\varepsilon_{eq} = (\alpha_{eq} - 1) \times 10^3$, which is 41.15‰ at 20 °C and is sensitive to temperature according to $\varepsilon_{eq} = 17604/K - 17.93$ (where K is temperature in Kelvins and $d\varepsilon_{eq}/dT = -0.2‰\ °C^{-1}$). Note that in nature, the $\delta^{18}O$ value of water involved in the CO_2–H_2O isotopic exchange also varies in a complex way, due to evaporative enrichment at the surface and pattern variations in the $\delta^{18}O$ of precipitation over time and space (Allison, 1982; Allison et al., 1987; Barnes and Allison, 1983a,b; Mathieu and Bariac, 1996a,b; Gat, 1996).

Importantly, the hydration reaction depicted in Eq. (2) is catalyzed by the enzyme carbonic anhydrase (CA), which is ubiquitous in leaves (Gillon and Yakir, 2001; Yakir, 2002) but can also exist in soils (Kesselmeier et al., 1999). While the uncatalyzed reaction is relatively slow (turnover of minutes), CA accelerates this reaction by many orders of magnitude. During diffusion of CO_2, for example, from the site of reaction, a kinetic isotope effect is also associated with the different diffusion rates of the isotopically labeled CO_2 molecules (Chapman and Cowling, 1970):

$$\alpha_{diff} = \frac{D_{(CO^{18}O)}}{D_{(CO_2)}} = \sqrt{\frac{(M_{CO^{18}O} + M_{air}) \cdot M_{CO_2}}{(M_{CO_2} + M_{air}) \cdot M_{CO^{18}O}}} \quad (4)$$

where D is the effective diffusivity and M is the molecular weight of the molecule. For CO_2 diffusion in air, the ^{18}O fractionation factor is 0.9913, which is often expressed as $\varepsilon_{diff} = (\alpha_{diff} - 1) \times 10^3$ (i.e., −8.7‰).

1.3. Invasion effect

As discussed above, the $\delta^{18}O$ of soil water influences the isotopic composition of the respired CO_2. But it also affects the isotopic composition of any atmospheric CO_2 which comes in contact with soil water, such as from CO_2 diffusing into and out of the soil. This abiotic process was termed atmospheric *invasion* (Tans, 1998; Miller et al., 1999; Stern et al., 2001). Depending upon its residence time in the soil, atmospheric CO_2 that diffuses into soil can partially or fully equilibrate with the soil water. Stern et al. (2001) assessed the importance of these abiotic fluxes to the global budget

of atmospheric δ^{18}O. Their estimates suggest that the magnitude of the abiotic CO_2 fluxes is significant and can be larger than 25% of the global soil–atmosphere respiratory flux, and therefore represent a significant effect on atmospheric δ^{18}O budget.

A general mathematical approach to understanding the process of invasion was developed by Tans (1998) and applied in an experimental system by Miller et al. (1999). Considering a chamber with a known height of air above the soil, the continuity equation is

$$\frac{dC_{out}}{dt} = \frac{1}{\tau_{air}}(C_{in} - C_{out}) + \frac{P}{h} \tag{5}$$

where C_{in} and C_{out} are the CO_2 concentrations in the incoming and outgoing air flowing through the chamber, and τ_{air} is the CO_2 mean residence time [s] in the chamber. The term P/h represents the contribution of soil respiration to the mass balance, where P is the production rate of respiration [mmol m^{-2} h^{-1}], and h is the height of the well-mixed air above the soil surface [m].

Eq. (5) ignores the fact that CO_2 diffuses into and out of the soil continuously, irrespective of the production term. The diffusing C_{in} has the opportunity to equilibrate with the soil water to an extent determined by the residence time and the efficiency of the invasion process. Adding this effect and the δ^{18}O corresponding to each CO_2 component, Eq. (5) can be expanded to yield (Miller et al., 1999):

$$\begin{aligned}\frac{d(\delta^{18}O_{out}\cdot C_{out})}{dt} &= \delta^{18}O_{out}\cdot\frac{dC_{out}}{dt} + C_{out}\cdot\frac{\delta^{18}O_{out}}{dt}\\ &= \frac{1}{\tau_{air}}(\delta^{18}O_{in}C_{in} - \delta^{18}O_{out}C_{out})\\ &\quad + \frac{v}{h}(\delta^{18}O_{eq} - \delta^{18}O_{out})\cdot C_{out} + \frac{P\delta^{18}O_P}{h}\end{aligned} \tag{6}$$

where $\delta^{18}O_{eq}$ is the δ^{18}O value of CO_2 isotopically equilibrated with soil water, and v is the efficiency of CO_2 diffusion, hydration and isotopic exchange in the soil (often termed piston velocity) which can be described by:

$$v = \sqrt{\theta_a B \theta_w \kappa D_0 K_H} \tag{7}$$

where θ_a and θ_w are the soil air and water volumetric content, respectively. The Bunsen coefficient, B, is defined as the molar density of the dissolved gas in water divided by the molar density in air (Weiss, 1974), and given by Tans (1998) as

$$B = 1.739\exp(-0.039T + 0.000236T^2) \tag{8}$$

where T is temperature of the liquid phase in °C. The rate constant for oxygen isotopic equilibrium of CO_2 and water is K_H, the tortuosity factor κ (discussed comprehensively in Section 3.1.2) is equal to about 0.66, and D_0 is the molecular diffusivity of CO_2 in free air (0.14 cm^2 s^{-1}; Hillel, 1980). Note that even when the soil is fully saturated and $v = 0$, an isotopic reaction between CO_2 and free water on the surface is still possible (see below and Fig. 3a).

For steady state conditions (under which our experiments were carried out), and substituting Eq. (5) into Eq. (6) yields:

$$\begin{aligned}&\delta^{18}O_{in}C_{in} - \delta^{18}O_{out}C_{in} + \frac{v}{h}\tau_{air}(\delta^{18}O_{eq} - \delta^{18}O_{out})C_{out}\\ &\quad + \frac{P}{h}\tau_{air}(\delta^{18}O_P - \delta^{18}O_{out}) = 0\end{aligned} \tag{9}$$

Eq. (9) is simplified significantly, at least in controlled experiments, by eliminating any production (i.e., $P = 0$). This removes any concentration (but not isotopic) gradients from the system, and consequently diffusion fractionation, so that any change in δ^{18}O can be assigned only to the effect of invasion:

$$\delta^{18}O_{in}C_{in} - \delta^{18}O_{out}C_{in} + \frac{v}{h}\tau_{air}(\delta^{18}O_{eq} - \delta^{18}O_{out})C_{out} = 0 \tag{10}$$

This expression is further simplified by defining $\tau_{inv} = h/v$, and the explicit contribution of the invasion effect, I, as $I = \frac{\tau_{air}}{\tau_{inv}}(\delta^{18}O_{eq} - \delta^{18}O_{out})$. Thus I can be derived in the simplified system, as done in this study, according to

$$\delta^{18}O_{out} = \frac{C_{in}\cdot\delta^{18}O_{in}}{C_{out}} + I \tag{11}$$

and therefore,

$$\begin{aligned}I &= \delta^{18}O_{out} - \frac{C_{in}\cdot\delta^{18}O_{in}}{C_{out}} = \delta^{18}O_{out} - \delta^{18}O_{in}\\ &= \Delta(\delta^{18}O)\end{aligned} \tag{12}$$

Note that Eq. (11) does not include surface effects that can occur when the soil is saturated, notably, the CO_2–H_2O exchange that can take place without invasion. Such a surface effect was included in the present version of the numerical simulation (see below and Fig. 3) by including the molecular diffusivity of CO_2 in water (2×10^{-5} cm^2 s^{-1}); the contribution of this diffusivity is often neglected because it is orders of magnitude smaller than the diffusivity in air (0.14 cm^2 s^{-1}).

The discussion above outlines an approach to address specifically the invasion effect. This simplified approach allows convenient experimental testing of the many assumptions and parameterizations associated with predicting the effect of soil on the δ^{18}O of atmospheric CO_2. It is important to recognize, in this respect, that insights gained from specific investigation of the invasion effect will apply also to production-enabled systems and thus help reduce uncertainties in the overall estimate of the δ^{18}O in the soil–atmosphere exchange flux. For example, both during invasion and production, CO_2 must diffuse within the wet soil along some minimal pathway that will provide the time required for isotopic equilibrium between CO_2 and water to take place (a process that occurs continuously along the soil profile). The soil depth at which this requirement is satisfied depends on the competing processes of diffusion (which can remove CO_2 from the soil) and the isotopic exchange reaction (which impacts the ^{18}O signal), and, of course, any factor that affects those processes, such as soil water content, soil structure and temperature. This issue has become a critical point because the δ^{18}O of soil water can be extremely variable near the soil surface due to evaporative enrichment (Mathieu and Bariac, 1996a,b). Therefore, in drying soils, uncertainties with respect to the depth of effective equilibrium between CO_2 and water that influence the ^{18}O content

of soil CO_2 efflux can constitute the largest uncertainty in the application of ^{18}O as a tracer for soil atmosphere CO_2 fluxes (Allison, 1982; Miller et al., 1999; Riley et al., 2002, 2003; Riley, 2005).

The objective of this study was to apply a combination of numerical simulations and experimental measurements to a simplified system of abiotic CO_2 invasion into soils. The idea was to separately and quantitatively assess the factors influencing the invasion effect, in general, and the depth of the effective CO_2–water isotopic equilibration in soils that influence the ^{18}O content in soil efflux, in particular.

2. MATERIALS AND METHODS

2.1. Dynamic flow-through chamber

A schematic diagram of the experimental apparatus is shown in Fig. 1; it was based on the design of Fang and Moncrieff (1996) and was the same system adapted and used by Miller et al. (1999). The chamber was fit on top of a closed box with inner dimensions of 20 cm × 22.3 cm × 22.3 cm. A seal between the two parts was made by using an O-ring and tightening with screws. The intake and outlet tubes had diameters of 19 mm and 4 mm, respectively, and together with "muffler" type inlets, were designed to prevent laminar flow and pressure differences higher than 0.2 Pa, as discussed in more detail in Miller et al. (1999).

2.2. Experimental porous media

The porous media used in the study consisted of clean, sieved sands (UNIMIN, USA). These sands are well-rounded quartz sand grains with minimal surface coatings (99.8% pure SiO_2, as reported by the manufacturer). The properties of the sand are given in Table 1 (Levy and Berkowitz, 2003).

Before use in experiments, the sand was rinsed with deionized water and oven dried for 48 h at 105 °C. After 4 h of cooling inside closed containers, measured quantities of water with known isotopic composition were homogenized with measured quantities of sand (used for soil moisture determinations) for 12 h, with manual mixing every ~3 h in closed containers to avoid evaporation. Sand samples were taken at the start and end of experiments (by using a test tube of 15 mm OD as a corer, and then immediately sealing it with the sample inside), and the actual mean sand water values during the experiments was −26.2‰. The evaporative effects for the ensuing short duration experiments reported here were small, with a mean difference in sand water (top 3–4 cm) between start and end of each experiment, for five consecutive experiments, of 0.27 ± 0.26‰. The sand water content, tested by coring soil in the experimental box, was found to be uniform up to water content of >50%, when water drainage to the bottom was observed.

2.3. Experimental procedure

The wetted sand was added homogeneously into the gas exchange system prior to commencing experiments that lasted ~4 h. Before sealing the chamber, a magnetic stir-bar was placed on the chamber ceiling with a magnetic stirrer placed on the chamber top and run at the lowest speed, to prevent development of laminar flow inside the chamber. The entire chamber was leak-tested using a non-dispersive infrared gas analyzer (IRGA, Li-Cor 6262, and Gashound) and pure CO_2. The chamber intake air was pumped (Robbins & Mayer diaphragm pump) from a 200 L covered plastic barrel located on the roof of the building, to prevent fluctuations in the CO_2 concentration during experiments. Samples of intake air were taken through a split in the supply air, before entering the chamber, using a diaphragm pump (Charles Austen) at a flow rate of 50–80 mL min^{-1}, regulated with a mass flow controller (MKS, 0–100 mL min^{-1}) that sucked the air through a dryer ($Mg(ClO_4)_2$) and 0.25 L glass flask high vacuum stopcock (Gas Expansion, Australia). Air dryness was checked with dewpoint measurement using the IRGA.

Airflow through the chamber was regulated with a mass flow controller (MKS, 0–5 L min^{-1}). Outlet air was sampled similarly to the inlet air, on a split from the main air hose. The two IRGAs mentioned above were connected to measure the inlet/outlet CO_2 (and H_2O) concentrations continuously throughout each experiment. Sampling of inlet/outlet air was done during steady state conditions, which was determined after a ~2–3 h stabilization period from stability of the CO_2 concentrations and by comparing C_{inlet} and C_{outlet} (and the stability over time of their $\delta^{18}O$ values). Precision of the CO_2 concentration measurements was ±0.1 and ±0.2 ppm for the Li-6262 and Li-800 (GasHound) instruments, respectively, but because ambient air was used (through a large buffer, see above) slow trends in [CO_2] over an experiment lasting several hours could result in standard deviations among samples from the same experiments of 1–4 ppm. Similarly, the differences in [CO_2] between the inlet and outlet during these experiments were, on average, 3.1 ± 1.7 ppm and were considered in the framework of Eq. (12). The experiments were carried out at constant room temperature of 25 °C (±1 °C). Due to the use of ambient air, the $\delta^{18}O$ value of the inlet air varied slightly over time and was on average −1.2 ± 0.1‰.

2.4. Forest site

Extension to more realistic field conditions was carried out in the Yatir forest in Israel (Grünzweig et al., 2003). Data from the long-term CarboEuroflux field site at Yatir (see http://www.carboeurope.org/) were used for porosity, soil water content, and soil temperature (from March 2002 to March 2003) at different depths. The Yatir site is a semi-arid pine afforestation system located in southern Israel where the soil type is light Rendzina (Haploxeroll) above chalk and limestone, with clay to sandy-clay-loam texture 33% clay, 21% silt, and 46% sand. Average soil temperature was 19.5 °C, and ranged between 9 and 32 °C with continuous 1/2 h data available since 2001. Volumetric water content was on average 16% and ranged between 4% and 30%, with data available on about a weekly basis.

2.5. Isotopic analysis

The $\delta^{13}C$ and $\delta^{18}O$ of CO_2 in air was analyzed using a continuous flow mass spectrometer configuration with a 15 flask automatic manifold system. An aliquot of 1.5 mL of air was expanded from each flask into a sampling loop on a 15-position valve (Valco). CO_2 was cryogenically trapped from the air samples using helium as a carrier gas; it was then separated from N_2O with a Carbosieve G packed column at 70 °C, and analyzed on a Europa 20-20 Isotope Ratio Mass Spectrometer. $\delta^{13}C$ results are quoted in parts per thousand (‰) relative to the V-PDB international standard (Coplen, 1994). The analytical precision was ±0.1‰.

The CO_2 isotopic composition of dry cylinder air obtained in Israel was calibrated locally and for each cylinder, samples were tested by sample inter-comparison with NOAA-CMDL, Boulder, Colorado, USA (cf. Trolier et al., 1996), with precisions of 0.1 ppm and 0.01‰.

Sand was extracted from samples taken with a plastic corer (test tube of 15 mm OD) by vacuum distillation at 80 °C. $\delta^{18}O$ values were determined by equilibration of 0.5 mL water with CO_2 for

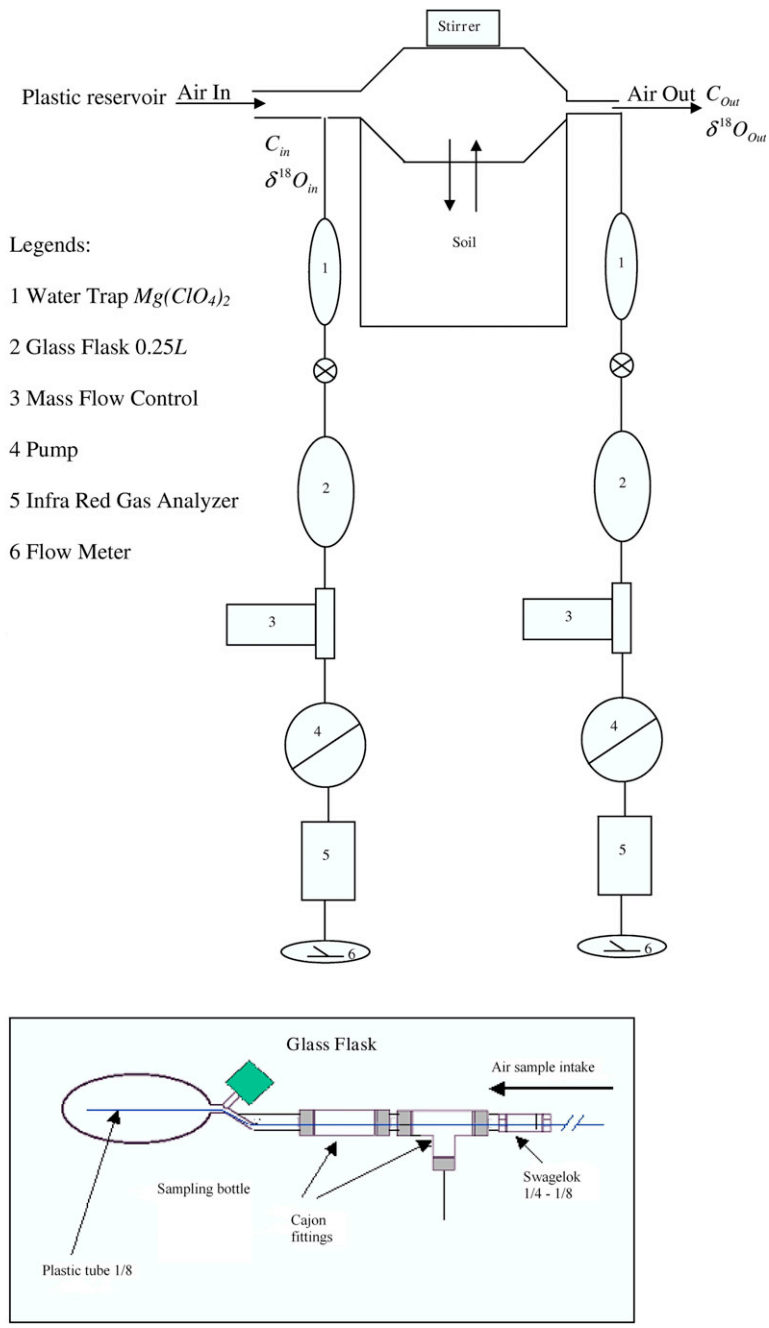

Fig. 1. Schematic of the dynamic soil gas exchange chamber used in this study.

Table 1
Properties of sands used in the experiments

Mesh size	Porosity (ϕ)	Grain diameter (mm)	Hydraulic conductivity (cm s^{-1})
50/70	0.376	0.231	0.014
12/20	0.370	1.105	0.500

24 h at 29 °C followed by cryogenic purification of a CO_2 aliquot. $\delta^{18}O$ values of the CO_2 were measured by dual inlet isotope ratio mass spectrometer (IRMS; MAT250, Finnigan, Bremen, Germany). Values were calibrated on the V-SMOW scale by simultaneously measuring an internal water standard (having a $\delta^{18}O$ value of −4.5‰ periodically calibrated to the international V-SMOW standard obtained form the IAEA, Vienna). Precision of the water mass spectrometric analysis was ±0.1‰.

2.6. Model formulation

A one-dimensional numerical model was designed to simulate production and diffusion of CO_2 in a soil profile, together with the exchange of ^{18}O between soil water and CO_2. The mathematical formulation was based on general principles derived by

Hesterberg and Siegenthaler (1991) and expanded later by Tans (1998).

The conceptual picture is of a well-mixed atmospheric reservoir of known height, which is flushed at a certain rate, lying above the soil. The soil characteristic profiles (i.e., water content, porosity, temperature, $\delta H_2{}^{18}O$ and production) are known in space and time, either from measurements or by assumptions. The concentration and isotopic composition of CO_2 were chosen to be the variables; they were solved by the numerical model described below.

The change in the CO_2 concentration in soil is described by the diffusion equation:

$$\frac{\partial(\theta_t C)}{\partial t} = \frac{\partial}{\partial z}\left(D_S \frac{\partial C}{\partial z}\right) + P \tag{13}$$

where $\theta_t = \theta_a + B\theta_w$ is the total CO_2 porosity (Tans, 1998), D_s is soil diffusivity, z is the soil depth, and t is the time (note that in the present study $P = 0$ and CO_2 concentrations are essentially homogeneous). The equation for the rate of isotopic species, as formulated by Hesterberg and Siegenthaler (1991) and Tans (1998), is:

$$\frac{\partial(\theta_t \mathrm{RC})}{\partial t} = \frac{\partial}{\partial z}\left[D_{iso}\frac{\partial(\mathrm{CR})}{\partial z}\right] + PR_S + K_H B\theta_w C(R_{eq} - R) \tag{14}$$

where D_{iso} is the molecular diffusivity of $C^{18}OO$ and is based on the gas diffusion in porous media. The ratio of isotopic species is expressed as $C(z)R(z)$, in which $R(z)$ is the ratio of the rare isotopic species to the total concentration of the chemical species, and $R_{eq}(z)$ is the isotopic ratio of CO_2 in equilibrium with soil moisture at local temperature. The factor $K_H B\theta_w$ represents the overall rate of isotopic equilibrium, which takes place only in the dissolved phase, with the CO_2–H_2O rate of isotopic equilibrium (due to oxygen scrambling in the carbonate ion) being:

$$K_H = \frac{H_{rate}}{3} \tag{15}$$

The hydration rate is given by Skirrow (1975) as

$$H_{rate} = 0.037\exp\left\{-9600\left(\frac{1}{273.15+T} - \frac{1}{298.15}\right)\right\} \tag{16}$$

The V-PDB value of CO_2 equilibrated with water is

$$\delta_{eq} = \delta_{H_2O} - 0.21(T - 25) \tag{17}$$

Note that δ_{H2O} of water in this equation is expressed relative to SMOW, whereas δ_{eq} (for CO_2) is expressed relative to V-PDB (a common approach to avoid the need to include the H_2O–CO_2 fractionation factor, see Eq. (3)), and T is the temperature of the liquid phase in °C.

The diffusivity D_S is a characteristic of the soil and depends strongly on the water content and temperature, as well as on other mechanical properties (i.e., soil structure). Two functions that are widely used to describe the diffusion coefficient in soil include the models of Penman (1940) and of Moldrup et al. (see Moldrup et al., 1999). The Penman model can be described according to:

$$D_S = D_0\kappa(\theta_S - \theta_w)\sqrt{\frac{T + 273.15}{298.15}} \tag{18}$$

where θ_s is the saturation water content of the soil, and using the small temperature correction as suggested in Tans (1998). This function is used in the numerical simulations throughout this study, unless otherwise indicated.

The second function is based on the model of Moldrup et al. (1999) according to

$$D_S = D_0\kappa\theta_S\left(\frac{\theta_S - \theta_w}{\theta_S}\right)^3\left(\frac{273.15 + T}{298.15}\right)^n \tag{19}$$

where T is the soil temperature in °C, and n should be 1.5 for the temperature range expected in soils (Riley et al., 2002; Bird et al., 2002). Irrespective of the diffusion model used, the ^{18}O diffusion coefficient is given by $D_{iso} = \alpha_{diff} D_S$, where α_{diff} is the kinetic fractionation (equal to 0.9913 based on the reduced mass equation of CO_2 isotopes in air, Eq. (4)). Note that a variation of Eq. (19) is given by Moldrup et al. (2003):

$$D_S = D_0(\theta_S - \theta_w)^2\left(\frac{\theta_S - \theta_w}{\theta_S}\right)^{3/b}\left(\frac{273.15 + T}{298.15}\right)^n$$

where b is the slope of the water retention curve (T in °C). This expression was considered by Riley (2005), who noted that use of this alternative expression has negligible impact on the predicted $\delta^{18}O$ value of the net soil-surface CO_2 flux.

Both carbon dioxide and isotopic fluxes at the surface ($z = 0$) can be determined at the atmosphere-soil boundary according to Fick's law, but in our experiments, at steady state and no production, there was only isotopic net flux:

$$F_{CO_2} = -D_S\frac{\partial C}{\partial z}$$
$$F_{18} = -D_{iso}\frac{\partial(\mathrm{CR})}{\partial z} \tag{20}$$

The model neglects advection of soil gas. Stern et al. (1999) examined the sensitivity of advection on the diffusion–production–reaction equation. Their results showed that advection is significant only in extreme cases of highly permeable soils combined with high frequency surface pressure variations resulting from strong winds. Note also that in the model used here, the diffusivity of CO_2 in water (2×10^{-5} cm^2 s^{-1}) is included, so that diffusion reduces to this factor rather than zero when the sand is fully saturated with water and there is no diffusion in air. This effect is usually ignored, because it is considered negligible compared to diffusion in air. As discussed below, this diffusivity results in a small surface effect, which is likely underestimated because of the assumption of a flat surface.

Boundary and initial conditions are specified to complete the model formulation. The CO_2 concentration, the isotopic composition of CO_2, and the fluxes F_{CO_2} and F_{18} depend on the soil characteristic profiles. A constant limit is assumed to simulate the soil characteristics:

$$P_{z,t=0} = P_{z,t=\infty} = 0$$
$$\theta_{z,t=0} = \theta_{z,t=\infty}$$
$$T_{z,t=0} = T_{z,t=\infty} \tag{21}$$
$$\delta H_2{}^{18}O_{z,t=0} = \delta H_2{}^{18}O_{z,t=\infty}$$

In addition, an impermeable boundary is imposed to simulate a soil profile with a closed base (at z = bottom):

$$F_{CO_{2(z=\mathrm{bottom},t)}} = 0$$
$$F_{18_{(z=\mathrm{bottom},t)}} = 0 \tag{22}$$

The initial conditions are simply

$$C_{z,t=0} = C_{atmosphere}$$
$$\delta^{18}O_{z,t=0} = \delta^{18}O_{atmosphere} \tag{23}$$

The above model was solved numerically. The main variables, CO_2 concentration and $\delta^{18}O$, were defined for every discrete depth. The soil was divided into discrete intervals of identical thickness, $z_0 = 0$ at the surface and $z_k = z_{max}$ at the lower boundary, for a total of 81 segments (see Fig. 2). The resolution of the diffusion–production equations consists of determining C and $\delta^{18}O$ at each time step. The equations were solved numerically with the method of implicit differencing (Press et al., 1992), which gives the correct steady-state solution of particular interest in this study.

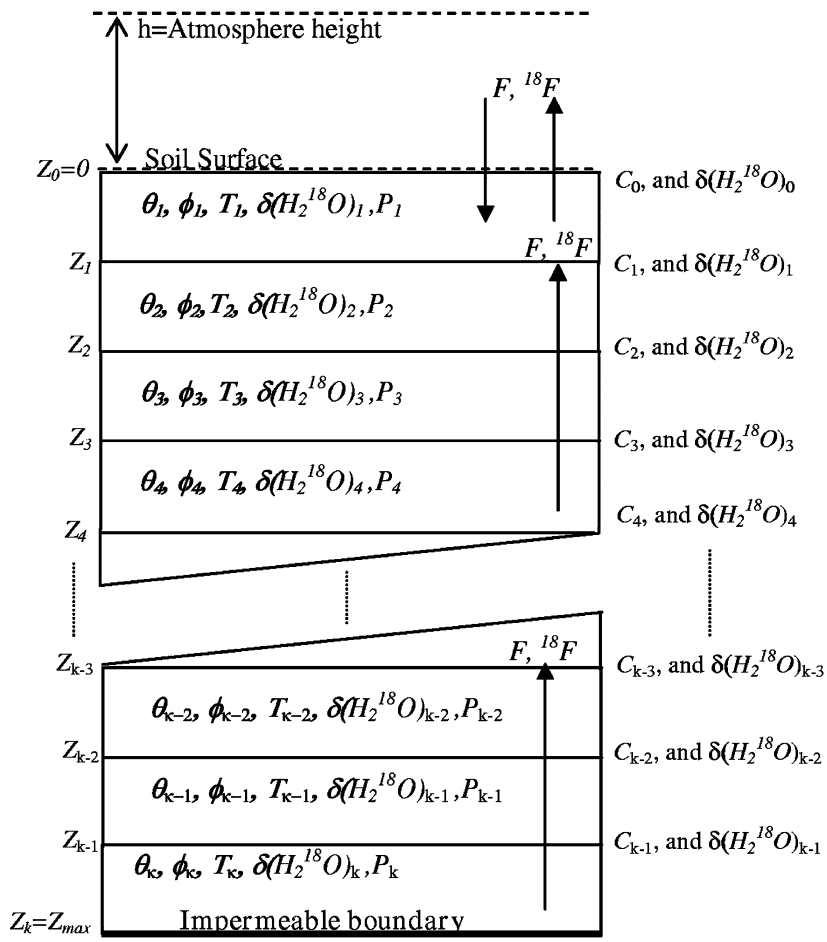

Fig. 2. Diagram showing the space discretization and the main variables in the numerical model. The following variables were used in all the model simulations: $\phi = 0.376$, $\delta H_2{}^{18}O_{soil} = -25‰$, $\delta CO^{18}O_{ambient} = -0.5‰$, $P = 0$ (μmol m^{-2} s^{-1}), $[CO_2] = 380$ ppm, $z = 20$ cm, residence time = 620 s, flow rate $q = 0.5$ L min^{-1}, $h = 10.5$ cm, $T = 25$ °C.

2.7. Model validation

The numerical isotopic exchange model was previously validated successfully (Tans, 1998) for simple comparisons of the simulated steady state solution concentration gradients and fluxes to the exact mathematical solutions of the equations that were obtained by using Green's functions (for respiration as an exponential function of depth, constant respiration with depth, and constant production underneath an inert surface layer).

Miller et al. (1999) subsequently provided experimental validation, checking the model against actual δ^{18}O measurements in soil air and effluxes. They found generally good agreements but with simulated δ^{18}O heavier by an average of 0.8‰. This was apparently due to the choice of a constant production function, which did not decrease with decreasing water content near the surface.

We first examined the influence of the time and space discretization on the CO_2 flux, and in particular, on the invasion. No effect of time discretization on the steady state solutions was found for time steps of 10 s, 100 s and 1000 s. Moreover, the calculated δ^{18}O of CO_2 profiles were almost identical for the relevant experimental soil column depths, i.e., 20, 30, 40 cm, with a spatial discretization of 81 segments. Variations of less than 0.2‰ appeared only for short residence times, and at the beginning of the simulations, using a strong isotopic signal of −25‰.

3. RESULTS AND DISCUSSION

We focused our study on the invasion effect, *I*, in abiotic systems, which we characterized in Section 1.3. In other words, we considered the δ^{18}O behavior of atmospheric CO_2, which is influenced by passive diffusion of atmospheric CO_2 into and out of wet soil, and the associated ^{18}O exchange between the CO_2 and the soil water. We expected that because of the association among diffusion, dissolution and exchange reaction, factors influencing these processes would affect *I*. Using numerical simulations, we explored the effect of soil moisture content, the choice of diffusion coefficient function, the CO_2 residence time, and the soil temperature on the magnitude of *I*. These simulations helped assess the relative importance of the various factors under a range of conditions that can be encountered in natural environments. A simplified experimental system was then considered, in which any biotic CO_2 production, and consequently any CO_2 concentration gradients and kinetic isotopic fractionation, were eliminated. We used experimental measurements to test our simulation parameterization, in particular to determine which of the two diffusion coefficient functions best fits the observations.

3.1. Numerical simulations

3.1.1. Soil moisture content

Our simulations clearly demonstrate the effect of invasion in wet soils on atmospheric CO_2. This is reflected in the decrease of the $\delta^{18}O$ values as the CO_2 passes over a wet soil; the extent of the change is dictated by the ^{18}O-depleted soil water. Because no CO_2 production or consumption was prescribed in our simulations, and because there is no change in CO_2 concentration or in any other condition with time, the $\delta^{18}O$ of soil water is the only factor that can drive the change in the $\delta^{18}O$ of the CO_2. For any given $\delta^{18}O$ of soil water, however, the magnitude of this effect is influenced by the amount of water in the soil (Fig. 3a). The effect of invasion is only noticeable if some moisture is present, and initially it increases with increasing soil moisture content. This is expected because water is the reactant in the exchange reaction (for the sake of convenience, we hereafter use the volumetric water content or water-filled void space, θ_v where $\theta_v = \theta_w/\theta_a$). At medium θ_v values, the effect of increasing θ_v diminishes, and there is little sensitivity to θ_v (depending on the choice of diffusion coefficient function, discussed below); at higher θ_v values, I actually decreases. This diminishing effect of θ_v on I is also expected because water-filled soil pores hinder the diffusion of CO_2 into the soil, and therefore the opportunity for CO_2–H_2O isotopic exchange during the prescribed residence time of the CO_2 in the systems (chamber flow rate in our experiments).

Note, however, that I does not vanish even at full soil saturation, i.e., for $\theta_v = 1$, $I \approx -0.3‰$ is observed (Fig. 3a). This surface effect, due to CO_2 dissolution and isotopic exchange with wet surface (see Section 2), is likely underestimated here as it assumes a flat wet surface. In reality, the actual soil surface roughness can increase such surface effects by an order of magnitude (i.e., potentially to an apparent I of $\sim -3‰$). This surface effect, as noted above, is due to some air CO_2 dissolving in the water, and some dissolved CO_2 leaving the water. For the experimental conditions, we estimate that about 0.4% of the air CO_2 could probably exchange with surface water, per minute; this corresponds roughly to the rate constant of hydration.

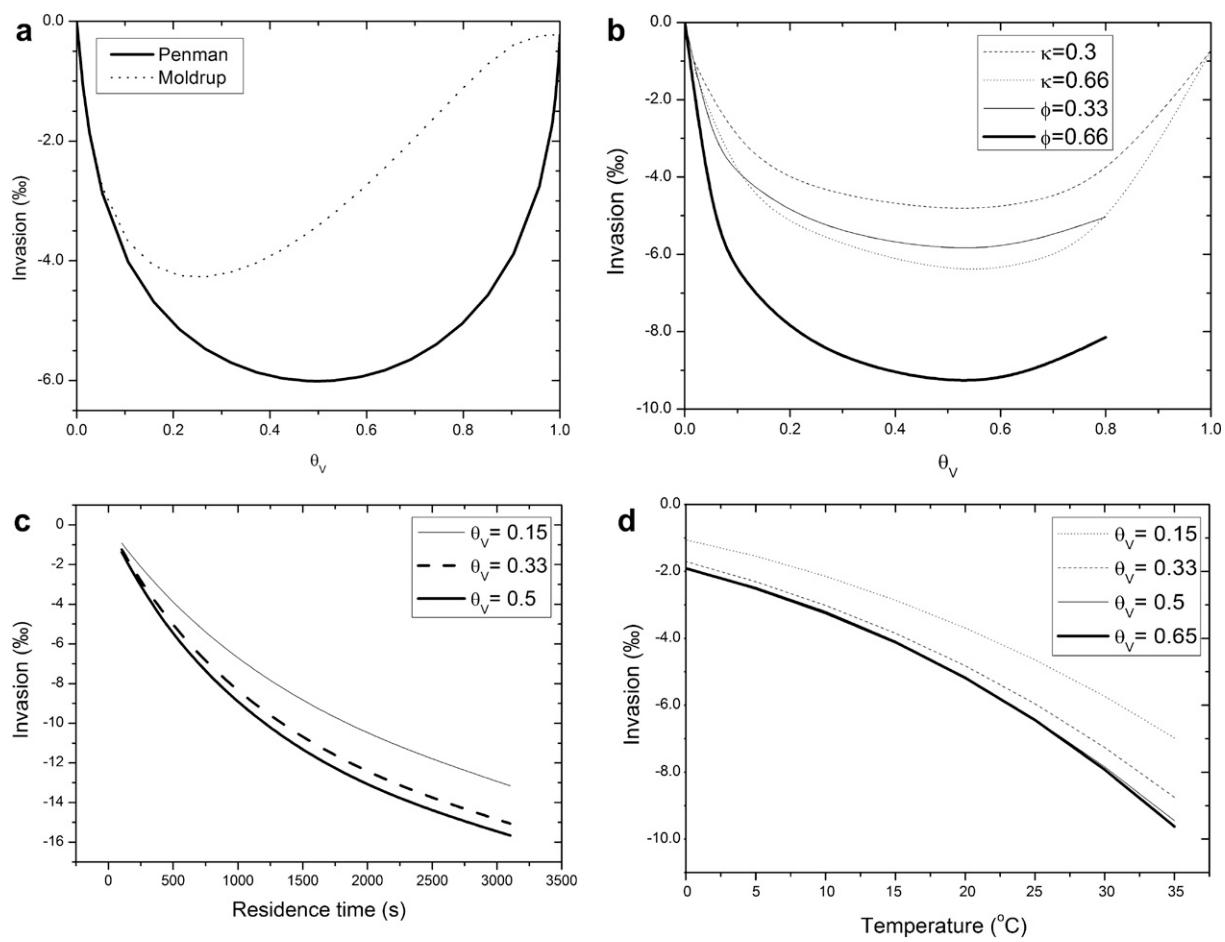

Fig. 3. Simulation predictions of invasion: (a) Invasion as a function of volumetric water content, for the diffusion coefficient functions of Penman (1940) and Moldrup et al. (1999). (b) Invasion as a function of soil physical properties (i.e., porosity and tortuosity) for various volumetric water contents. (c) Invasion as a function of residence time for various volumetric water contents. (d) Invasion as a function of temperature for various volumetric water contents. Simulations were based on Eqs. 13, 14 (with no production term) and the parameters indicated in Fig. 2.

3.1.2. Diffusion coefficient function

As discussed above, increasing the soil water content affects invasion both by enhancing the exchange rate, because more reactant is available, and by inhibiting exchange, because diffusion pathways are blocked. Riley et al. (2002, 2003) and Riley (2005) pointed out that in numerical simulations, the rate of CO_2 diffusion in soils is greatly influenced also by the choice of diffusion coefficient function; these functions incorporate the effects of porosity and temperature in different ways. Two commonly used models, namely the Penman (1940) model (Eq. (18)) applied by Miller et al. (1999), Tans (1998), Mathieu and Bariac (1996b) and Stern et al. (1999), and the Moldrup et al. (1999) model (Eq. (19)), considered by Riley et al. (2002, 2003), produced different predictions of the invasion effect. Notably there are many other studies that consider various ways to estimate the diffusivity parameter, and for different media and ambient conditions. Here we chose only two approaches that have been selected in previous studies, and apply them to a simplified synthetic experimental system.

Fig. 3a demonstrates how these two models predict the response of I to changes in θ_v. For very low volumetric water contents, similar I values were obtained with the two diffusion models (Fig. 3a), but for θ_v greater than about 10%, the differences increase to a maximum of ~4‰ at $\theta_v \approx 80\%$. The range of reduced sensitivity of I is over $\theta_v \approx 10$–50% when using Eq. (18), but over $\theta_v \approx 30$–80% when using Eq. (19) (Fig. 3a). The relatively large differences between the predicted I values for the two diffusion models provide an opportunity to test these two representations of diffusion experimentally. This test is discussed below.

A complex parameter factored into the diffusivity coefficient models is the tortuosity, κ. The concept behind this parameter is to scale the diffusion distances in porous media. It is common to estimate the tortuosity in sand as $\kappa = 0.66$ (Hillel, 1980), but in much finer textured materials, the value of tortuosity can decrease to $\kappa = 0.2$ (Barnes and Allison, 1988). Mathieu and Bariac (1996b) used $\kappa = 0.49$ for a porosity $\phi = 0.55$ based on Philip (1957). In Fig. 3b we considered a realistic range of porosity and tortuosity values and examined their effects on I. The effects of different porosity and tortuosity values on I are comparable. However, note that porosity tends to be inversely proportional to tortuosity and, hence, porosity increases as tortuosity decreases. Interestingly, the results obtained here indicate that I is not very sensitive to the combined effects of porosity and tortuosity. But in contrast, Stern et al. (2001) indicated that I can vary for different sites with very different soil types. We show below that I can also vary in similar soils with different grain size. It thus appears that the low sensitivity reported here applies in particular to variations in porosity/tortuosity for the same soil type and grain size, but more significant changes in soil type and grain size (e.g. different sites) would influence I more strongly.

3.1.3. CO_2 residence time

In both model simulations and experimental measurements, reported below, the flow rate of air above the soil surface determined the residence time of the CO_2 in contact with the wet soil. Longer residence times expose the CO_2 to additional active sites. This parameter influenced (together with the soil parameters) the time available for CO_2 to diffuse into the soil, react, and equilibrate isotopically with soil water. Clearly, longer residence times are expected to enhance the invasion effect, as indeed observed in the model simulations (Fig. 3c). Note, however, that the pattern of the residence time effect is not linear and the effect diminishes with increasing residence time values. Ultimately, it is expected that the $\delta^{18}O$ of CO_2 will approach the equilibrium value with soil water (−25‰ for Fig. 3, after considering temperature effects; cf. Eq. (17)). Under natural conditions, the residence time for invasion is influenced by the turbulence conditions near the soil surface, and long residence times are expected at night and in dense canopies, which are associated with high concentrations of air CO_2 due to soil respiration.

3.1.4. Temperature

Two competing processes are involved in the invasion effect, namely CO_2 diffusion and reaction (which occurs only while the CO_2 is in wet soil). Variations in soil temperatures, in the range normally encountered in nature, affect the diffusion coefficient function negligibly. But such variations strongly influence the hydration rates, and consequently the rate of exchange of oxygen isotopes between CO_2 and soil water.

Fig. 3d demonstrates the effect of temperature on I, based only on calculating its effect on the hydration rate of CO_2 (Eq. (16); based on Skirrow, 1975), and its consequent effect on the rate of CO_2–H_2O isotopic equilibrium (Eq. (15)). The temperature effect on I is large, even within the range commonly encountered in ecosystems over the diurnal and seasonal cycles (as noted also by Stern et al., 1999). The influence of soil moisture content on the temperature response, however, is relatively small. For example, a 10 °C temperature change, in the range of 20–30 °C, results in an almost 3‰ change in I. This is a much larger effect than expected, for example, when compared to short-term changes in soil moisture content or changes in CO_2 residence time in turbulent air (Fig. 3a and c). This effect can be expected because increasing temperature effectively reduces the depth required for CO_2 diffusion to attain equilibrium enrichment in ^{18}O. Therefore, variations in temperature associated with changes in $\delta^{18}O$ of soil water with depth can produce significant changes in I on daily and seasonal time scales, irrespective of any other changes.

3.2. Experimental validation of the diffusion coefficient model

As noted by Riley (2005); see also Riley et al. (2002, 2003) and discussed above (Fig. 3a), the choice of diffusivity coefficient function is a subject of debate, but the expected differences should allow experimental testing of the more suitable function. Here, we employed a simplified experimental system using the methodology used by Miller et al. (1999). We eliminated production and consumption of CO_2 and used a large difference in $\delta^{18}O$ between soil water and CO_2 with $d(\delta^{18}O_{H_2O})/dz = 0$ to examine the fits

of the two diffusivity coefficient models of Penman (1940) and Moldrup et al. (1999) to the patterns of the ^{18}O exchange, as expressed in the invasion effect.

Note that a simple ratio between Eqs. (18) and (19) yields approximately the term $(\frac{\theta_S-\theta_w}{\theta_S})^2 \frac{273.15+T}{298.15}$ which is near unity for low soil water contents (i.e., $\theta_w \ll \theta_a$ under the same soil temperatures), but not at high θ_w values, consistent with the simulations presented in Fig. 3a. However, other than for dry soils the experimental results for the response of I air flow-rate (i.e., CO_2 residence time) and to θ_w, shown in Fig. 4a and b, respectively, are fit well only by the simulations based on the Penman model. Listed in order of significance the results can be summarized as follows. (1) Good agreement is found between the Penman (1940) diffusivity coefficient function and experimental results, both in predicting the response to changes in θ_v and to residence time (Fig. 4a and b). The Moldrup et al. (1999) function consistently predicts smaller I values for the same conditions. (2) Using the Penman function, a better correlation with experimental results is observed at higher θ_v values (>30%). This may be due to higher experimental error and difficulties in producing homogeneous soil samples in the lower range of θ_v. (3) Residence time plays an important role in both experimental and simulated results. Residence time is a prescribed parameter and can influence the results and interpretations, but simulations showed that this effect is significant only at extremely low flow rates (e.g., ~0.1 L min^{-1}; in Fig. 3b). (4) Measurements of $\Delta(\delta^{13}C)$ (i.e., $\Delta(\delta^{13}C) = \delta^{13}C_{out} - \delta^{13}C_{in}$) were used as a control for the ^{18}O measurements, because no change in $\delta^{13}C$ values was expected during the abiotic flow-through experiments. Values of $\Delta(\delta^{13}C)$ were on average (for all experiments) -0.3 ± 0.5‰, with no response to the variables used, supporting the notion that the $\Delta(\delta^{18}O)$ from which I values are derived was not influenced significantly by the experimental setup. (The residual ^{13}C effect was consistent with some residual CO_2 production observed in our stored sand reserves, but during experiments it was associated with a minor CO_2 gradient across the soil box during experiments (see Section 2, and Eq. (11)) and was considered insignificant.) (5) All experiments were carried out with pure sand of relatively uniform grain size. Possible effects of grain size and structure on the water–CO_2 exchange or the invasion effect were not considered. This point was checked separately, as discussed below.

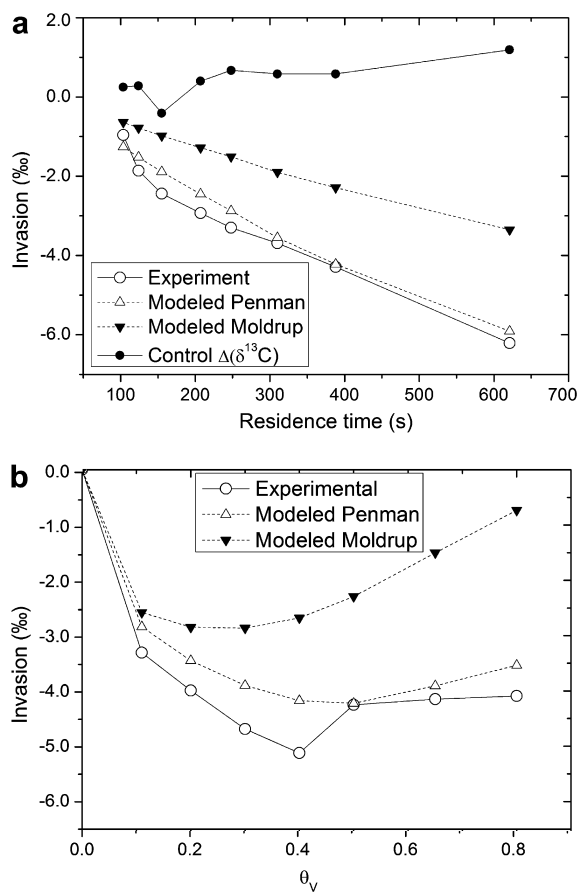

Fig. 4. Experimental results on model validation: (a) Invasion as a function of residence time for $\theta_v = 50\%$. (b) Invasion as a function of volumetric water content for residence time of 388 s (i.e. chamber flow rate of 0.8 L min^{-1}). Parameter values are specified in Fig. 2 except: $\delta H_2{}^{18}O_{soil} = -26.2$‰, $\delta CO^{18}O_{ambient}$ = varying, $[CO_2]$ = varies 370–405). The simulations were based on solving numerically Eqs. 13, 14, 18, 19 and experimental results were used with Eq. (11) (note there was no production term in this study). The ^{13}C control in a was based on $\Delta(\delta^{13}C) = \delta^{13}C_{out} - \delta^{13}C_{in}$.

Low (1979) showed that physical properties, such as the nature of hydrogen bonds formed by bound water, specifically interlayer water in montmorillonite clay, differ from properties of bulk water (Isaac, 2001). Isaac (2001) reported that the large surface to volume ratio imposed on soil water could enhance significantly the isotopic hydration reaction rate. Miller et al. (1999) envisaged that water adsorbed to surfaces probably contains ^{18}O bound more strongly than when in solution, and as a result the kinetic fractionation decreases. In our study we used rounded quartz sand with minimal surface coatings, generally assuming that water is predominantly unbound, except for hydrogen bonding between water molecules. We examined experimentally the effects of using sand with different grain diameters, and therefore different properties such as surface area, but with otherwise identical chemical properties (including porosity). The results of four independent measurements (Fig. 5a and b) showed that I was always greater for fine grain sand than for coarse sand (by 0.7–1.2‰, and on average 1.2 ± 1.0‰). Although more measurements are needed, it seems this structural effect was stronger in dry soils, and that it rapidly diminishes with increasing soil water content (Fig. 5). This is consistent with the idea that the isotopic reaction between water and CO_2 occurs predominantly on thin films surrounding particle surfaces, rather than in bulk water.

3.3. Depth of ^{18}O equilibrium

A major issue associated with estimating exchange of ^{18}O between CO_2 and water in wet soils is associated with the common observation of a large isotopic gradient in soil water at the top ~5 cm of the soil, which is due to evaporative enrichment (Mathieu and Bariac, 1996a; Miller et al., 1999; Riley, 2005). If the effective depth of isotopic equili-

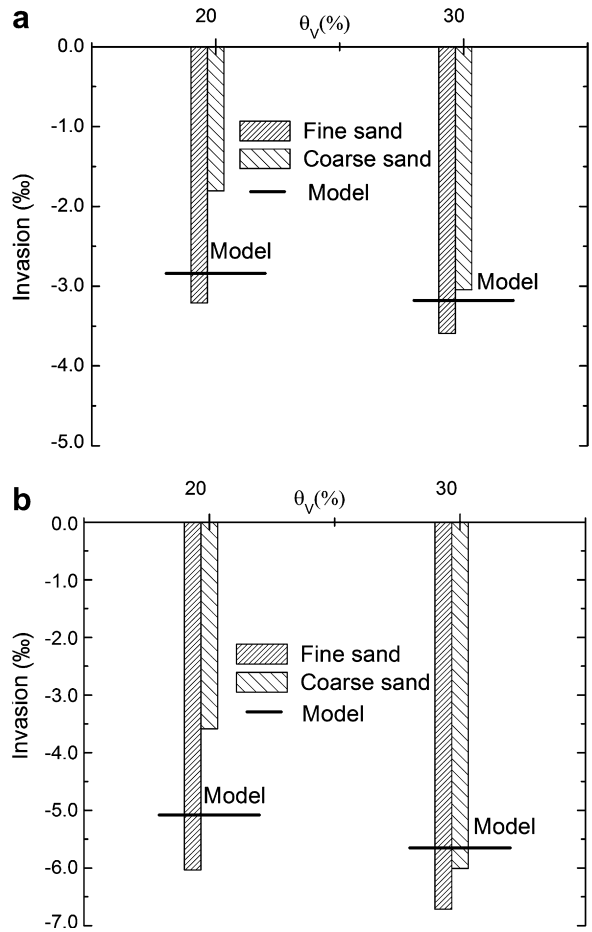

Fig. 5. Experimental results from four independent measurements showing the effects of grain size on invasion under volumetric water content of 20% or 30%, and (a) residence time of 310 s (=chamber flow rate of 1 L min^{-1}), or (b) residence time of 620 s (=chamber flow rate of 0.5 L min^{-1}). Parameter values as in Fig. 2 except: $\delta H_2{}^{18}O_{soil} = -26.2‰$, $\delta CO^{18}O_{ambient}$ = varying, $[CO_2]$ = varies 370–405.

bration that is reflected in the ^{18}O of the soil CO_2 efflux is near the surface, such isotopic enrichment must be considered in predicting the δ^{18}O of soil–atmosphere CO_2 exchange flux. If, on the other hand, the effective depth of isotopic equilibrium is below the large enrichment depth, predictions are significantly simplified and can rely on precipitation data.

The effective equilibration depth (realizing that exchange occurs anywhere there is CO_2 and water in the soil), which will be reflected in the ^{18}O content of the soil CO_2 efflux, depends on the competing rates of diffusion of CO_2 out of the soil and of CO_2 hydration and isotopic exchange. Miller et al. (1999) estimated, experimentally, an effective "setting point depth" (SPD, see Miller et al., 1999 for detail) based on empirically matching the δ^{18}O of soil respired CO_2 (biotic processes) with the water δ^{18}O along the soil profile in the top 20 cm in soils undergoing evaporation. They found SPD in the range of about 5–15 cm, and a mean of ~7 cm. These experiments were conducted in drying soils, which increase the soil diffusivity coefficient (see above) and yield deeper SPDs than in wet soils. Nonetheless, the range of θ_w values in these experiments is commonly observed in field studies and much smaller SPDs could not be predicted for these conditions. In contrast, based on numerical simulations and using the Moldrup equation, Riley et al. (2003) and later Riley (2005, using both Moldrup and Penman equations) contradicts the observations of Miller et al. (1999) that the δ^{18}O value of water in the top five centimeters of soil does not substantially impact the δ^{18}O value of the soil-surface CO_2 flux. It was argued that this was consistent, for example, with a decrease in the measured δ^{18}O value of soil respired CO_2 following a small precipitation event that did not penetrate the upper soil layer of (0–2.5 cm).

In the simplified experimental setup used in this study, no production and soil water isotopic gradient existed, and numerical and analytical approaches were used to approximate the effective depth of ^{18}O equilibration in the soil associated with CO_2 invasion process (abiotic). The lack of isotopic gradient in the soil profile precluded the estimate of SPD as done in previous studies. As a consequence, an equivalent parameter is used to estimate the depth to which CO_2 must diffuse in the soil to allow sufficient time for full isotopic equilibrium (termed the "full equilibration depth", FED, see below).

3.3.1. Numerical estimates of the full equilibrium depth of ^{18}O

Numerical simulations were used to determine the δ^{18}O value of CO_2 along the soil profile at the top 20 cm. As noted above, we define the full equilibrium depth (FED) as the depth to which CO_2 must diffuse in the soil to allow sufficient time for full isotopic equilibrium. We evaluate this numerically as the point in which the difference in δ^{18}O between soil CO_2 and water was equal or smaller than 0.3‰ (a threshold chosen for practical purposes to represent the overall precision of the measurements). FED is distinguished from the empirically estimated SPD of Miller et al. (1999), which used the ^{18}O gradient in soil water that did not exist here. While SPD can be assessed only in the presence of gradients, FED can be assessed in both cases and provides a similar means to estimate the efficiency of equilibrium vs. diffusion. Fig. 6 shows the FED simulation results for various temperatures and water contents. The results show the expected trends of decreasing FED with increasing either θ_v (Fig. 6a) or temperature (Fig. 6b). The simulations also show that for the abiotic invasion process, as represented by FED approaches zero only at very high θ_v or temperature values, as predicted by Riley et al. (2002, 2003). For conditions commonly encountered in the field, however, the depths are equivalent to those predicted by Miller et al. (1999) for their soil samples. Note that for very dry or very cold soils, the full equilibrium depth can be considerable.

3.3.2. Analytical estimates of the full equilibrium depth of ^{18}O

An independent approach is taken as an order of magnitude check on the numerical simulation of FED. This is based on using simplified analytical estimates and comparing the characteristic times for CO_2 diffusion in the soil column

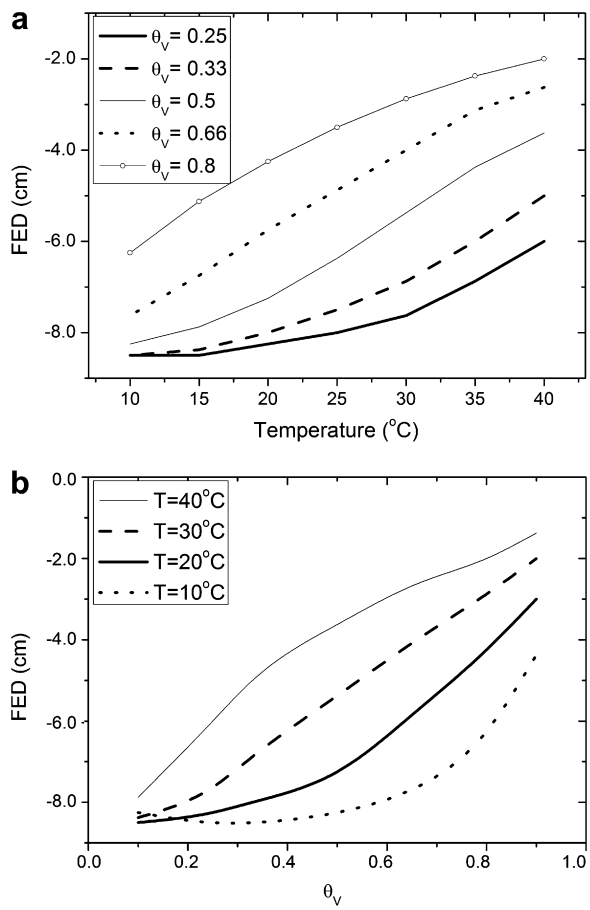

Fig. 6. Simulation predictions of full equilibration depth (FED). The FED was defined as the point in which the difference in $\delta^{18}O$ between soil CO_2 and water was equal to or smaller than 0.3‰ (approximately the experimental error in the measurements), and was obtained from $\partial\delta(CO_2)_{k=bottom}/\partial\delta(CO_2)_k = 0.3‰$) and $\delta(CO_2)_{k=bottom}$ and $\delta(CO_2)_k$ were the equilibrium and FED values, respectively. (a) FED as a function of volumetric water content for various soil temperatures. (b) FED as a function of temperatures for various soils volumetric water contents. Parameters used in the simulations were as specified in Fig. 2.

and for the isotopic reaction between CO_2 and soil water. Following Weisz (1973) for different applications we use:

$$\rho = \frac{t_{iso-h}}{\tau} \tag{24}$$

where ρ here is ratio between the time required for hydration–isotopic exchange reaction, t_{iso-h}, and the characteristic time, τ, required for CO_2 to diffuse through a soil column of length L. When $\rho = 1$, the gas diffuses a sufficient time to allow isotopic equilibration. The kinetics, half-life for isotopic equilibrium of CO_2 in soil water is a first-order reaction and can be described by

$$\frac{\ln 2}{K_H} = t_{iso-h} \tag{25}$$

where K_H is defined by Eq. (15). The relationship between the distance L traveled by CO_2 molecules and the diffusion time, τ, for diffusion in soil, is

$$\tau = \frac{\overline{L^2}}{2\,D_S} \tag{26}$$

We employ the approach used also by Miller et al. (1999) and Riley (2005) but using the Penman (1940) diffusion model based on the results discussed above. We first compare the solution for the required reaction time in water, ρ, based on the ratio between Eqs. (25) and (26) (Fig. 7a). The solution can also be given for the various distances required to attain this reaction time in a given soil, and the net distance traveled by CO_2 molecules:

$$\overline{L} = \sqrt{\frac{2D_S \ln(2)}{K_H}} \tag{27}$$

The results are summarized in Fig. 7a, which considers the characteristic time for CO_2 diffusion through a range of possible soil column lengths, and the half-life for isotopic equilibrium of CO_2 soil water. A point at which a depth line and reaction time line meet indicates the minimum soil depth required to attain full isotopic equilibrium, given the conditions indicated. Thus, points to the left of the reaction time line represent combinations that would allow full isotopic equilibrium and to the right of this line, combinations in which CO_2 would escape the soil without full equilibrium. Note that these analytical solutions are distinct from the empirical approach of Miller et al. (1999), but are based on the same principles and provide "first approximations" that can be used as another check on empirical or (as used here) on numerical simulations. As expected, using the Moldrup model (Fig. 7b) instead of the Penman model (used in Fig. 7a) yields significantly smaller simulated equilibration depths. For example, taking $k_{iso-h} = 0.012\ s^{-1}$, $T = 25\ °C$, $\phi = 37.6\%$, $B = 0.76$, $\kappa = 0.66$, and moderate θ_v (25–40%) yields required soil depths of 4 cm and 2 cm, instead of 8 cm and 6 cm, based on the Moldrup and Penman approaches, respectively. Note that this analytical approach gives a relatively large domain, because the characteristic time for diffusion represents the time for the midpoint of diffusive plume to propagate a particular distance in a medium; and the characteristic time for hydration characteristic represents the half-life of hydration reaction.

Comparing the results of the numerical and the analytical approaches discussed above (Figs. 6a and 7a, respectively), we find generally good agreement for comparable soil conditions (Fig. 7c). This is reassuring, but note that the correlation deteriorates at low water content. This is likely because the analytical solution for equilibration time approaches infinity at very low water contents (see Fig. 6a), while the numerical simulation does not.

3.3.3. Seasonal variations in the depth of full equilibrium

To further extend our analyses to more realistic field conditions, we used available annual-scale data from the Yatir forest (see Section 2) to estimate the FED (which applies either to atmospheric invasion flux, or to a production flux that would exist under field conditions). We calculated the full equilibration time, using a harmonic averaging of layered diffusion coefficients according to Crank (1975):

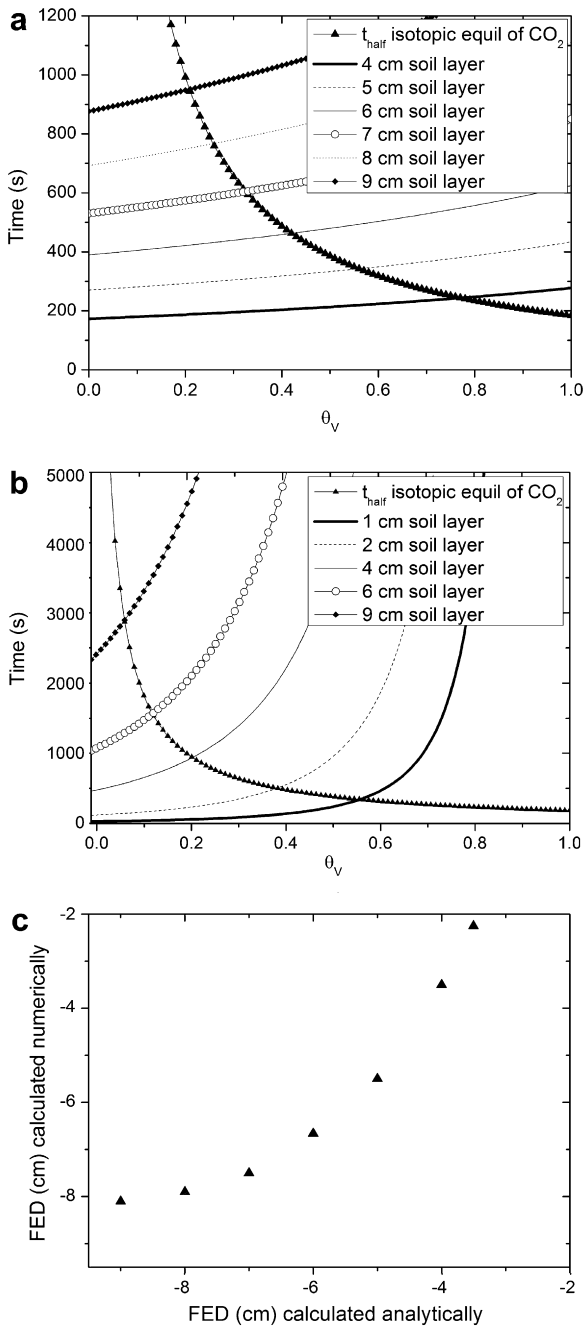

Fig. 7. (a) Characteristic times for isotopic hydration-equilibrium and diffusion, across soil columns of varying lengths (based on Penman (1940; using equations 15–16, 18–19, 25–26, $T = 25$ °C) (b) As for (a), but based on the Moldrup et al. (1999) model. (c) Comparison of the full equilibration depth (FED) between analytical solution (a) and numerical solution (b).

$$\frac{1}{D_S} = \sum_{i=1}^{n} \frac{1}{D_S(\phi_i, \theta_w, T_i)} \tag{28}$$

The analytical and numerical estimates of FED were almost identical in the ranges between −2.5 cm and −8 cm (see Fig. 7c) and in the following analysis we used the analytical approach as described in Section 3.3.2.

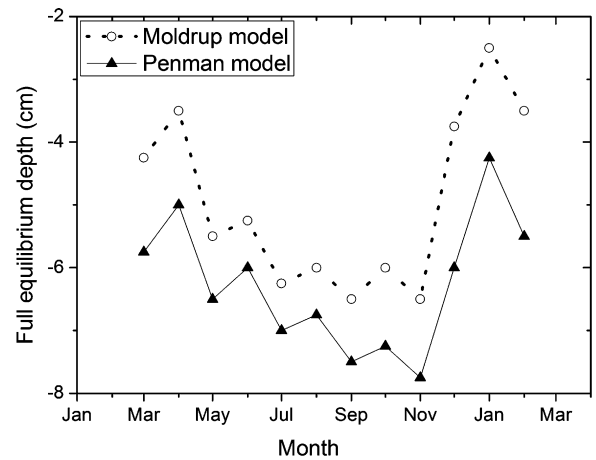

Fig. 8. Seasonal variations, between March 2002 and March 2003, of the full equilibration depth (FED) using the Penman (1940) and Moldrup et al. (1999) diffusion coefficient functions.

The results summarized in Fig. 8 show significant seasonal variation in the predicted full equilibration depth for this site, with the expected deepening of the equilibration depth in the dry summer (see Hesterberg and Siegenthaler, 1991). The full equilibration depth observed ranged between ~4 cm in winter (January) and ~7.5 cm in autumn (November) for estimates based on the Penman model. Using the Moldrup model, the trends are similar but with shallower depths of ~2.5 cm in the winter (January) and ~6.5 cm in autumn (November). As noted by Miller et al. (1999), these seasonal variations tend to help reduce the effect of evaporative enrichment near the soil surface as the soil dries up. In other words, the full equilibrium depth increases as the near-surface enrichment intensifies.

Using the Penman diffusion model, the average full equilibrium depth in Yatir was 6.27 ± 1.05 (while the average depth using the Moldrup model was 4.96 ± 1.39), in good agreement with Miller et al. (1999) for different environments (Colorado) and based on biotic CO_2 production. The results indicate that such estimates are relatively robust, as least for mid-range θ_w values. This also supports the notion that at least in such soils, the ^{18}O enriched water often observed in the top ~5 cm of drying soils (Allison, 1982; Allison et al., 1983, 1987; Barnes and Allison, 1983, 1984; Kroopnic and Craig, 1972; Mathieu and Bariac, 1996a,b) is not expected to impart a strong isotopic signature to the CO_2 escaping the soil, unless, of course, CO_2 is produced at or near the surface or carbonic anhydrase exists at these sites.

4. CONCLUSIONS

We used a simplified experimental system combined with numerical model simulations to explore the factors that influence the depth of ^{18}O equilibrium between CO_2 and soil water. Our approach relied on abiotic exchange only, with no production/consumption, and using homogeneous sand with no variations in the δ^{18}O of soil water. We used a gas exchange system similar to that of Miller et al. (1999).

We show, in order of importance, that: (1) I is sensitive to soil moisture content and its isotopic composition, temperature, CO_2 residence time, and to soil structure (porosity, tortuosity and grain size). (2) Numerical simulations of these effects are sensitive to the diffusion coefficient function used; good agreement between experimental measurements and predictions using numerical simulations was obtained using both the Penman and the Moldrup diffusion equations for soil with low water content, but only with the former for soil with intermediate and high water content. (3) Based on the preferred Penman model, numerical simulations and field data indicate that the depth of full CO_2–H_2O equilibrium in the soil profile normally ranges between ~2 cm and ~8 cm with a mean depth of ~6 cm. (4) Using the field data, seasonal variations show significant deepening of the full equilibrium depth in summer, thus reducing the soil surface effect when it is most expected to undergo large evaporative enrichment (this analysis was based on comparison of characteristic times). (5) All else being equal, I is greater for fine sand than for coarse sand at low water contents, suggesting that I is dependent on the wet surface area in the soil.

These results support the idea that the competition between CO_2–H_2O isotopic exchange, and CO_2 diffusion out of the soil, limits the effect of near-surface isotopic enrichment of soil water on the $\delta^{18}O$ of the soil–atmosphere CO_2 flux, simplifying the prediction of its effect on atmospheric CO_2. We note however that our study focused only on abiotic invasion and does not consider various patterns of biological CO_2 production and enzyme catalyzed exchange about the soil surfaces. The results provide additional insights to the recent advances in understanding the effects of soil on the isotopic composition of the global atmosphere (Stern et al., 1999; Miller et al., 1999; Riley et al., 2002, 2003).

ACKNOWLEDGMENTS

We gratefully acknowledge financial support from the US-Israel Binational Science Foundation (BSF-2000-293), and from the Minerva Foundation. We thank Emanuela Negreanu for the IRMS measurements, Reuven Dagan for technical help in chamber constructions, Matan Levy and Vasile Turcu for helpful discussions, and Dr. Jose Grünzweig for providing the Yatir soil measurement data. We also thank Dr. Cole and three anonymous reviewers for their useful comments.

REFERENCES

Allison G. B. (1982) The relationship between ^{18}O and deuterium in water in sand columns undergoing evaporation. *J. Hydrol.* **55**(1–4), 163–169.

Allison G. B., Colin-Kaczala C., Filly A., and Fontes J. C. (1987) Measurements of isotopic equilibrium between water, water vapor and soil CO_2 in arid zone soils. *J. Hydrol.* **95**, 131–141.

Barnes C. J., and Allison G. B. (1983a) The distribution of deuterium and ^{18}O in dry soils 1. Theory. *J. Hydrol.* **60**, 141–156.

Barnes C. J., and Allison G. B. (1983b) The distribution of deuterium and ^{18}O in dry soils 2. Experiment. *J. Hydrol.* **64**, 377–397.

Barnes C. J., and Allison G. B. (1988) Tracing of water movement in unsaturated zone using stable isotopes of hydrogen and oxygen. *J. Hydrol.* **100**, 143–176.

Bird R., Stewart W., and Lightfoot E. (2002) *Transport Phenomena*, second ed. John Willey, New York.

Blunier T., Barnett B., Bender M. L., and Hendricks M. B. (2002) Biological oxygen productivity during the last 60,000 years from triple oxygen isotope measurements. *Global Biogeochem. Cyc.* **16**(3). doi:10.1029/2001GB00146.

Brenninkmeijer C. A. M., Kraft P., and Mook W. G. (1983) Oxygen isotope fractionation between CO_2 and H_2O. *Isotope Geosci.* **1**, 181–190.

Chapman S., and Cowling T. (1970) *The mathematical theory of non-uniform gases*, Third ed. Cambridge University Press, Cambridge.

Conway T. J., Tans P. P., Waterman L. S., Thoning K. W., Kitsiz D. R., Massarie K. A., and Zhang N. (1994) Evidence for interannual variability of carbon cycle for National Oceanic and Atmospheric Administration/Climate Monitoring Diagnostics Laboratory Global Air Sampling Network. *J. Geophys. Res.* **99**(D11), 22831–22855.

Coplen T. B. (1994) Reporting of stable hydrogen, carbon and oxygen isotopic abundances. *Pure Appl. Chem.* **66**(2), 273–276.

Crank J. (1975) *The Mathematics of Diffusion*. Clarendon Press, Oxford.

Fang C., and Moncrieff J. B. (1996) An improved dynamic chamber technique for measuring CO_2 efflux from the surface soil. *Funct. Ecol.* **10**, 297–305.

Farquhar G. D., Lloyd J., Taylor J. A., Flanagan L. B., Syvertsen J. P., Hubick K. T., Wong S. C., and Ehleringer J. R. (1993) Vegetation effects on the isotope composition of oxygen in atmospheric CO_2. *Nature* **363**, 439–443.

Francey R. J., and Tans P. P. (1987) Latitudinal variation in oxygen-18 of atmospheric CO_2. *Nature* **327**, 495–497.

Gat J. R. (1996) Oxygen and hydrogen isotopes in hydrologic cycle. *Annu. Rev. Earth Planet. Sci.* **24**, 225–262.

Gillon J., and Yakir D. (2001) Influence of carbonic anhydrase activity in terrestrial vegetation on the ^{18}O content of atmospheric CO_2. *Science* **291**, 2584–2587.

Grünzweig J. M., Lin T., Rotenberg E., and Yakir D. (2003) Carbon sequestration in arid-land forest. *Global Change Biol.* **9**, 791–799.

Hemming D., and Yakir D.WP5 members (2005) Pan-European $\delta^{13}C$ signatures from forest ecosystems. *Global Change Biol.* **11**, 1065–1072.

Hesterberg R., and Siegenthaler U. (1991) Production and stable isotopic composition of CO_2 in a soil near Bern, Switzerland. *Tellus* **43B**, 197–205.

Hillel D. (1980) *Fundamental of Soil Physics*. Academic Press, San-Diego.

Isaac, M. (2001). The oxygen isotopic signal of CO_2 in low moisture soils, M.Sc. Thesis, Weizmann Institute of Science, Israel.

Keeling C. D., Chin J. F. S., and Whorf T. P. (1996) Increased activity of northern vegetation inferred from atmospheric CO_2 observation. *Nature* **382**, 146–149.

Kesselmeier J., Teusch N., and Kuhn U. (1999) Controlling variables for uptake of atmospheric carbonyl sulfide by soil. *J. Geophys. Res.* **104**(D9), 11577–11584.

Kroopnic P., and Craig H. (1972) Atmospheric oxygen-isotopic composition and solubility fractionation. *Science* **175**(4017), 54–55.

Levy M., and Berkowitz B. (2003) Measurement and analysis of non-Fickian dispersion in heterogeneous porous media. *J. Cont. Hydrol.* **64**(3-4), 203–226.

Mathieu R., and Bariac T. (1996a) An isotopic study (^{2}H and ^{18}O) of water movement in clayey soils under a semi-arid climate. *Water Resour. Res.* **32**(4), 779–789.

Mathieu R., and Bariac T. (1996b) A numerical model for simulation of stable isotope profiles in drying soils. *J. Geophys. Res.* **101**(D7), 12685–12696.

Miller J. B., Yakir D., White J. W. C., and Tans P. P. (1999) Measurements of $^{18}O/^{16}O$ in the soil atmosphere CO_2 flux. *Global Biogeochem. Cyc.* **13**(3), 761–774.

Moldrup P., Olesen T., Yamaguchi T., Schjonning P., and Rolston D. E. (1999) Modeling diffusion and reaction in soils, IX, The Backingham–Burdine–Campbell equation for gas diffusivity in undisturbed soil. *Soil Sci.* **164**, 542–551.

Moldrup P., Olesen T., Komatsu S., Yoshikawa P., Schjonning P., and Rolston D. E. (2003) Modeling diffusion and reaction in soils: X. A unifying model for solute and gas diffusivity in unsaturated soil. *Soil Sci.* **168**, 321–337.

Penman H. L. (1940) Gas and vapor movements in soil, 1: the diffusion of vapors through porous solids. *Int. J. Agric. Sci.* **30**, 437–462.

Philip J. R. (1957) Evaporation and moisture and heat fields in the soils. *J. Meteorol.* **14**, 354–366.

Press W., Teukolsky S., Vetterling W., and Flannery B. (1992) *Numerical Recipes*, second ed. Cambridge University Press, Cambridge.

Randerson J. T., Thompson M. V., Conway T. J., Fung I. Y., and Field C. B. (1997) The contribution of terrestrial sources and sinks to trends in seasonal cycle of atmosphere carbon dioxide. *Global Biogeochem. Cyc.* **11**(4), 535–560.

Riley W. J. (2005) A modeling study of the impact of the $\delta^{18}O$ value of near-surface soil water on the $\delta^{18}O$ value of the soil-surface CO_2 flux. *Geochim. Cosmochim. Acta* **69**(8), 1939–1946.

Riley W. J., Still C. J., Torn M. S., and Berry J. A. (2002) A mechanistic model of $H_2{}^{18}O$ and $CO^{18}O$ fluxes between ecosystems and the atmosphere: model description and sensitivity analysis. *Global Biogeochem. Cyc.* **16**(4). doi:10.1029/2002GB00187.

Riley W. J., Still C. J., Helliker B. R., Ribascarbo M., and Berry J. A. (2003) ^{18}O composition of CO_2 and H_2O ecosystem pools and fluxes in tallgrass prairie: simulations and comparisons to measurements. *Global Change Biol.* **9**, 1567–1581.

Skirrow, G. (1975). The dissolved gases-carbon dioxide. In *Chemical Oceanography*, vol. 2 (eds. J. P. Riley and G. Skirrow). Academic Press, San Diego, CA , pp. 1–92.

Stern L., Baisden W. T., and Amundson R. (1999) Processes controlling the oxygen isotope ratio of soil CO_2: analytic and numerical modeling. *Geochim. Cosmochim. Acta* **63**(6), 799–814.

Stern L., Amundson R., and Baisden W. T. (2001) Influence of soils on oxygen isotope ratio of atmospheric CO_2. *Global Biogeochem. Cyc.* **15**(3), 753–759.

Tans P. P. (1998) Oxygen isotopic equilibrium between carbon dioxide and water in soils. *Tellus* **50**(B), 163–178.

Trolier M., White J. W. C., Tans P. P., Massarie K. A., and Gemery P. A. (1996) Monitoring the isotopic composition of atmospheric CO_2 measurements from the NOAA global air sampling network. *J. Geophys. Res.* **111**(D20), 25897–25916.

Weiss R. F. (1974) Carbon dioxide in water and seawater: the solubility of non-ideal gas. *Marine Chem.* **2**, 203–215.

Weisz P. B. (1973) Diffusion and chemical transformation. *Science* **197**, 433–440.

Yakir D., and Wang X. F. (1996) Fluxes of CO_2 and water between terrestrial vegetation and atmospheric estimated from isotope measurements. *Nature* **380**, 515–517.

Yakir, D. (2003). Isotopic composition of atmospheric CO_2. *Treatise on Geochemistry*, vol. 4.07 (ed. R. Keeling). Elsevier, San Diego.

Yakir D. (2002) Global enzymes: sphere of influence—Concept. *Nature* **416**, 795.

Associate editor: David R. Cole